Published in final edited form as:
Ann N Y Acad Sci. 2011 December ; 1240: 47–52. doi:10.1111/j.1749-6632.2011.06237.x.

Measuring intranodal pressure and lymph viscosity to elucidate mechanisms of arthritic flare and therapeutic outcomes

Echoe M. Bouta[a,b], **Ronald W. Wood**[c,d], **Seth W. Perry**[b], **Edward Brown**[b], **Christopher T. Ritchlin**[a,e], **Lianping Xing**[a,f], and **Edward M. Schwarz**[a,b,d,e,f]

[a]Center for Musculoskeletal Research, University of Rochester School of Medicine and Dentistry, Rochester, NY

[b]Department of Biomedical Engineering, University of Rochester School of Medicine and Dentistry, Rochester, NY

[c]Department of Obstetrics and Gynecology, University of Rochester School of Medicine and Dentistry, Rochester, NY

[d]Department of Urology, University of Rochester School of Medicine and Dentistry, Rochester, NY

[e]Division of Allergy, Immunology, Rheumatology, Department of Medicine, University of Rochester School of Medicine and Dentistry, Rochester, NY

[f]Department of Pathology and Laboratory Medicine, University of Rochester School of Medicine and Dentistry, Rochester, NY

Abstract

Rheumatoid arthritis (RA) is a chronic autoimmune disease with episodic flares in affected joints, whose etiology is largely unknown. Recent studies in mice demonstrated alterations in lymphatics from affected joints precede flares. Thus, we aimed to develop novel methods for measuring lymph node pressure and lymph viscosity in limbs of mice. Pressure measurements were performed by inserting a glass micropipette connected to a pressure transducer into popliteal lymph nodes (PLN) or axillary lymph nodes (ALN) of mice and determined that the lymphatic pressures were 9 and 12 cm of water, respectively. We are also developing methods for measuring lymph viscosity in lymphatic vessels afferent to PLN, which can be measured by multi-photon fluorescence recovery after photobleaching (MP-FRAP) of FITC-BSA injected into the hind footpad. These results demonstrate the potential of lymph node pressure and lymph viscosity measurements, and warrant future studies to test these outcomes as biomarkers of arthritic flare.

Keywords

Rheumatoid Arthritis; Lymph Node; Flare; Lymphatic Pressure; Lymph Viscosity

Corresponding author: Dr. Edward M. Schwarz, The Center for Musculoskeletal Research, University of Rochester Medical Center, 601 Elmwood Avenue, Box 665, Rochester, NY 14642, Phone: 585-275-3063, Fax 585-275-1121, Edward_Schwarz@URMC.Rochester.edu.

Disclosures

Dr. Ronald Wood is an inventor of lymphatic imaging techniques that the University of Rochester has licensed to Novadaq Technologies, Inc.

Introduction

Rheumatoid arthritis (RA) is a debilitating immune-mediated inflammatory disorder characterized by joint inflammation and destruction, which affects 1% of the population[1]. Major advances in our understanding of pivotal events that underlie the pathobiology of RA have fostered the development of several biologic therapies that specifically target the inflammatory cytokines (TNF, IL-1, IL-6) and immune cells (B-cells, monocytes) implicated in synovitis and joint destruction. Despite these advances, several aspects of RA pathogenesis remain poorly understood. Foremost among them are the episodic flares and remissions observed in RA over the course of time. Joint flares are associated with significant morbidity and loss of function, so a major unmet need is the elucidation of flare mechanisms to catalyze new drug development for RA patients.

Murine models of acute and chronic RA, such as the KxRN serum induced arthritis (SIA)[2] and TNF transgenic mouse (TNF-Tg)[3] models respectively, have been very useful for elucidating the pathophysiology of inflammatory-erosive arthritis. Recently, inflamed joints in these models have been analyzed with contrast enhanced (CE) MRI. These imaging studies demonstrate that arthritic knee flare is associated with the expansion and subsequent collapse of the popliteal lymph node (PLN)[4–7], which drains inflamed joints[7]. This PLN collapse, i.e. reduction in lymph node volume, is accompanied by the migration of a subset of $CD21^{hi}/CD23^{+}/IgM^{hi}/CD1d^{+}$ B cells in inflamed nodes (Bin) into the paracortical sinuses and this centripetal movement is associated with blockage of the lymphatic vasculature: a process which is ameliorated by anti-CD20 B cell depletion therapy[6]. Additional alterations in lymphoid biology during inflammatory arthritis include increased VEGF-C dependent lymphangiogenesis[8, 9] and diminished lymphatic pulsation as determined by near infrared-indocyanine green (NIR-ICG) imaging[10]. Thus, a formal association between altered lymphatic volumes and variation in lymphatic flow and the onset of arthritic flare has been established. Unfortunately, methods to directly measure the lymphatic pressure and viscosity changes during and after arthritic flare and following therapy have not been established in animal models of RA.

To facilitate a better understand of lymph node pressure and lymph viscosity, we explored several *in vivo* imaging techniques in normal wild type (WT) mice. The results demonstrated that pressure can be measured using a glass micropipette connected to a pressure transducer, while viscosity measurements are feasible by using the Stokes-Einstein equation and calculating the diffusion coefficient following *in vivo* MP-FRAP.

MATERIALS AND METHODS

Animals

The female WT C57Bl/6 mice used in this study were purchased from Charles River Laboratories (Wilmington, MA). All mice were between 8–10 weeks old. During NIR-ICG imaging, animals were anesthetized with 1.5% isoflurane in oxygen. During MP-FRAP, animals were anesthetized with ketamine. The research was conducted with approval by the University of Rochester Medical Center Institutional Animal Care and Use Committee.

Pressure measurements

Mice were injected with 30μl of 1% Evan's blue (Sigma Aldrich, St. Louis, MO) in the hind footpad or front paw for initial visualization the PLN (n=8) or ALN (n=7), respectively. After ~20 minutes, the PLN or ALN was exposed via an incision through the overlying skin. An operating microscope (Op Mi6, Ziess, West Germany) was used to insert a luer lock borosilicate glass micropipette with an inner tip diameter of 30μm (World Precision Instruments, Sarasota, FL) into the PLN or ALN. The glass micropipette was filled with ICG

and attached to a pressure transducer (Sorenson Transpac IV, Abbott, North Chicago, IL) and infusion pump (PHD 2000, Harvard Apparatus, Holliston, MA) via polyvinyl chloride (PVC) tubing (Figure 1A). Correct placement was confirmed visually and by pumping ICG into the PLN through the micropipette and confirming it resided in the PLN and upstream lymphatics (Figure 1B). Pressure recording and control of ICG imaging parameters was achieved using customized software (LabVIEW; National Instruments, Austin, TX). If excessive leaking of ICG was detected (Figure 1C), indicating improper placement of the micropipette, data was discarded. Calibration of the glass micropipette and pressure transducer was preformed after each session manometrically.

Viscosity measurements by MP-FRAP

While FRAP has been used in biological systems to characterize flow[11, 12], MP-FRAP has the advantage of being able to be performed *in vivo* in real time[13]. Briefly, a laser is used to monitor the sample at a low power while keeping focal volume consistent throughout the experiment. Then, the sample is photobleached by a brief strong pulse of the laser, modulated through a Pockels' cell, to induce photobleaching. After the bleach, the laser power returns to the lower monitor power as the fluorescence recovers to baseline. Photons are collected by a photomultiplier tube and recorded throughout the experiment by a photon counter. Multiple monitor-bleach-recovery curves, performed in rapid succession, are summed to produce the final curve. Recovery is dependent on diffusion and convection. From the recovery curve after photobleaching, the diffusion coefficient and the flow rate can be determined. The diffusion coefficient is found by fitting the recovery curve to the following equation in Matlab (MathWorks, Natick, MA)[13, 14]:

$$F(t)=F_0\sum_{n=0}^{\infty}\frac{(-\beta)^n}{n!}\frac{\exp\left[\frac{-4n(t/\tau_v^2)}{1+n+2nt/\tau_D}\right]}{(1+n+2nt/\tau_D)(1+n+2nt/R\tau_D)^{1/2}}$$

where β is the bleach depth parameter, τ_v is a time constant due to flow, τ_D is a time constant due to diffusion and R is the square of the ratio of the axial to radial dimensions of the focal volume. From this, the diffusion coefficient (D) can be determined by[13, 14]:

$$D=w_r^2/8\tau_D$$

where w_r is the radius of the focal volume.

Viscosity, η, can be found from the diffusion coefficient by the Stokes-Einstein equation:

$$\eta=\frac{k_bT}{6\pi Dr}$$

where k_b is Boltzmann's constant, T is temperature and r is the hydrodynamic radius of FITC-BSA.

In our *in vivo* paradigm, MP-FRAP is first calibrated by measuring the *in vitro* diffusion coefficient of FITC-BSA in water. Because the viscosity of water is a constant, and FITC-BSA D values can be fit by models[13, 14], the relative FITC-BSA D values calculated *in vitro* (in water) versus *in vivo* (in lymph) can be used to ratiometrically calculate the viscosity of lymph via the Stokes-Einstein equation. This ratiometric approach may help minimize sources of experimental uncertainty in the final calculated lymph viscosity, compared to

calculating viscosity from the Stokes-Einstein equation alone based on a software-fitted *D* value for FITC-BSA in lymph (which in turn is dependent on lymph viscosity). The hind footpads of mice were injected with 30μl of FITC-BSA (Sigma Aldrich, St. Louis, MO) ≤ 2 hours before MP-FRAP measurements. Correct location of MP-FRAP was confirmed by imaging the lymphatic vessel via two-photon microscopy. Only curves with a smooth recovery and sufficient bleaching were used.

Statistical analysis

All results are presented as the mean ± standard deviation. Data was first checked for normality and groups were checked to have equal variances by the KS test and F-test, respectively. Comparisons between groups were analyzed by a two-tailed Student's *t*-test. *p* values less than 0.05 were considered significant.

RESULTS

The lymphatic pressure was measured in both popliteal and axillary lymph nodes of WT mice using the system described in Figure 1. The pressure of axillary lymph nodes was 11.70 ± 0.83 cm H_2O and was 25% greater than that observed in PLN (8.95 ± 0.73 cm H_2O) (Figure 2A).

Occasionally, a pulse could be detected in the pressure measurement (Figure 2B). This pulse rate (1 beat/30 seconds) is consistent with the known intrinsic lymphatic pulse that we observed using NIR imaging in mouse legs[10]. Although we did succeed in measuring the lymphatic pulse rate with our method, this approach will need to be markedly improved to detect it consistently, as it likely requires precise positioning of the glass micropipette within the lymphatic channels running through the lymph node. This can likely be achieved with a precise micromanipulator.

As described in Materials and Methods, the viscosity of lymph in lymphatic vessels afferent to PLN is determined *in vivo* by first measuring the diffusion coefficient of known standards *in vitro* (Figure 3A). Others have calculated the *in vitro* diffusion coefficient of FITC-BSA in water to be ~ 50 μm^2/second[13, 14]. *In vivo* MP-FRAP curves (Figure 3B) are then acquired from peri-valve regions of lymphatic vessels that have been filled with FITC-BSA by injecting the hind footpad (Figure 3C). We are presently working on adapting our computer modeling to obtain best-fits of fluorescent recovery *D* values for the *in vivo* lymphatic environment, but these results demonstrate that acquisition of MP-FRAP data from lymph vessels *in vivo* is feasible and should ultimately yield real-time values of lymph viscosity.

DISCUSSION

Here we describe novel methods quantify pressure in draining lymph nodes and viscosity in lymphatic vessels and PLN of mice, and propose that they will be helpful towards elucidating the mechanisms during and after arthritic flare and responses to therapy using various murine models of RA[15]. We hypothesize that both pressure of the lymph nodes and viscosity of lymph will increase during the pathogenesis of inflammatory arthritis. This pressure increase could be caused by the influx of macrophages and Bin cells into the draining lymph node[6], and the 5-fold increase in lymphatic pulsing[10]. Additional lymphatic pressure could be caused by a change in viscosity due bone and joint catabolism in which extracellular matrix breakdown products and minerals are cleared in lymph. While lymphangiogenesis and draining lymph node expansion are designed to counteract this pressure increase and prevent lymphatic vessel rupture, there is likely a threshold pressure that exceeds the capacity of these compensatory mechanisms. We hypothesize that when this

threshold pressure is achieved, it triggers shutdown of the lymphatic pulse, which results in the collapse of the draining lymph node. The resulting loss of lymphatic draining from the joint is manifested as an arthritic flare.

Despite its known importance as a biomarker of inflammation and tumor metastasis, very little has been done to measure the parameters of the murine lymphatic system because of the diminutive size of the animal compared to other species used for lymphatic investigations. Pressure has been measured in the lymphatic vessels and capillaries in humans, sheep and rabbits[16–18]. The measurement of lymphatic pressure in small mammals is scarce, but an early study measured pressure of lymphatic vessels in mouse ear[19]. However, there is no report of measuring lymphatic pressure in draining lymph nodes of mouse limbs where arthritis occurs. Recently, others have measured the pressure inside the human lymph node for detection of cancer cell metastasis in the lymph nodes. The study found that the intranodal pressure in sentinel lymph nodes without tumors was 9.1 ± 6.2 mmHg[20], very similar to our findings. Tumor-containing lymph nodes were found to have a pressure of 21.4 ± 15.4 mmHg; the rationale is that when more cells reside within the lymphatic vessels of a sentinel lymph node, it will increase overall pressure of the node.

Although we have no formal explanation for the difference in pressure seen between the ALN and PLN, one possible contributor is the remarkable difference in mass between the lymphatics of the lower vs. upper limbs of mice. As the volume of the lymphatics of the lower limb is apparently greater than the upper limb, we hypothesize that distribution over a greater surface area could result in lower pressure.

Others have measured the viscosity of lymph in dogs by collecting the lymph from the thoracic duct and using a viscometer. The viscosity of lymph was analyzed to determine if changes of lymph correlate with changes in diet[21]. Unfortunately, parallel approaches are not applicable in smaller animals where the lymphatic vessels cannot be cannulated, and low lymph volumes preclude application of typical methods to determine viscosity. MP-FRAP overcomes these constraints by using optical techniques, opposed to physically measuring the viscosity of the fluid in question. This allows the viscosity of the fluid to be found without being collected so the viscosity of lymph can be measured throughout the course of the experiment.

The methods described in this paper overcome the size constraints of measuring murine lymph node pressure and lymph viscosity. Pressure can be measured by inserting a glass micropipette into the PLN while the viscosity of lymph can be measured by MP-FRAP. Experiments designed to test our hypotheses that both lymph node pressure and lymph viscosity will increase during the pathogenesis of inflammatory arthritis are currently underway using the methods described here.

Acknowledgments

This work was supported by research grants from the National Institutes of Health PHS awards (T32 AR053459; R01s AR048697, AR053586 and AR056702; P01 AI078907; DP2OD006501; and P30 AR061307).

References

1. Firestein GS. Evolving concepts of rheumatoid arthritis. Nature. 2003; 423(6937):356–361. [PubMed: 12748655]
2. Kouskoff V, Korganow AS, Duchatelle V, Degott C, Benoist C, Mathis D. Organ-specific disease provoked by systemic autoimmunity. Cell Mol Bioeng. 1996; 87(5):811–822.

3. Keffer J, Probert L, Cazlaris H, Georgopoulos S, Kaslaris E, Kloussis D, Kollias G. Transgenic mice expressing human tumour necrosis factor: a predictive genetic model of arthritis. EMBO. 1991; 10(13):4025–4031.
4. Proulx ST, Kwok E, You Z, Beck CA, Shealy DJ, Ritchlin CT, Boyce BF, Xing L, Scharwz EM. MRI and quantification of draining lymph node function in inflammatory arthritis. Ann N Y Acad Sci. 2007; 1117:106–123. [PubMed: 17646265]
5. Proulx ST, Kwok E, You Z, Papuga MO, Beck CA, Shealy DJ, Ritchlin CT, Awad HA, Boyce BF, Xing L, Scharwz EM. Longitudinal assessment of synovial, lymph node, and bone volumes in inflammatory arthritis in mice by in vivo magnetic resonance imaging and microfocal computed tomography. Arthritis Rheum. 56(12):4024–4037. [PubMed: 18050199]
6. Li J, Kuzin I, Moshkani S, Proulx ST, Xing L, Skrombolas D, Dunn R, Sanz I, Schwarz EM, Bottaro A. Expanded CD23(+)/CD21(hi) B cells in inflamed lymph nodes are associated with the onset of inflammatory-erosive arthritis in TNF-transgenic mice and are targets of anti-CD20 therapy. J Immunol. 2010; 184(11):6142–6150. [PubMed: 20435928]
7. Guo R, Zhou Q, Proulx ST, Wood R, Ji RC, Ritchlin CT, Pytowski B, Zhu Z, Wang YJ, Schwarz EM, Xing L. Inhibition of lymphangiogenesis and lymphatic drainage via vascular endothelial growth factor receptor 3 blockade increases the severity of inflammation in a mouse model of chronic inflammatory arthritis. Arthritis Rheum. 2009; 60(9):2666–2676. [PubMed: 19714652]
8. Zhang Q, Lu Y, Proulx ST, Guo R, Yao Z, Schwarz EM, Boyce BF, Xing L. Increased lymphangiogenesis in joints of mice with inflammatory arthritis. Arthritis Res Ther. 2007; 9(6):R118. [PubMed: 17997858]
9. Zhou Q, Guo R, Wood R, Boyce BF, Liang Q, Wang YJ, Schwarz EM, Xing L. Vascular endothelial growth factor C attenuates joint damage in chronic inflammatory arthritis by accelerating local lymphatic drainage in mice. Arthritis Rheum. 2011; 63(8):2318–2328. [PubMed: 21538325]
10. Zhou Q, Wood R, Schwarz EM, Wang YJ, Xing L. Near-infrared lymphatic imaging demonstrates the dynamics of lymph flow and lymphangiogenesis during the acute versus chronic phases of arthritis in mice. Arthritis Rheum. 2010; 62(7):1881–1889. [PubMed: 20309866]
11. Kwon RY, Frangos JA. Quantification of Lacunar-Canalicular Interstitial Fluid Flow Through Computational Modeling of Fluorescence Recovery After Photobleaching. Cell Mol Bioeng. 2010; 3(3):296–306. [PubMed: 21076644]
12. Bonvin C, Overney J, Shieh AC, Dixon JB, Swartz MA. A multichamber fluidic device for 3D cultures under interstitial flow with live imaging: development, characterization, and applications. Biotechnol Bioeng. 2010; 105(5):982–991. [PubMed: 19953672]
13. Sullivan KD, Sipprell WH 3rd, Brown EB Jr, Brown EB 3rd. Improved model of fluorescence recovery expands the application of multiphoton fluorescence recovery after photobleaching in vivo. Biophys J. 2009; 96(12):5082–5094. [PubMed: 19527668]
14. Brown EB, et al. Measurement of molecular diffusion in solution by multiphoton fluorescence photobleaching recovery. Biophys J. 1999; 77(5):2837–49. [PubMed: 10545381]
15. van den Berg WB. Animal models of arthri*tis.* What have we learned? J Rheumatol Suppl. 2005; 72:7–9. [PubMed: 15660455]
16. Franzeck UK, Fischer M, Costanzo U, Herrig I, Bollinger A. Effect of postural changes on human lymphatic capillary pressure of the skin. J Physiol. 1996; 494:595–600. [PubMed: 8842016]
17. McGeown JG, McHale NG, Thornbury KD. The effect of electrical stimulation of the sympathetic chain on peripheral lymph flow in the anaesthetized sheep. J Physiol. 1987; 393:123–133. [PubMed: 3446793]
18. Negrini D, Del Fabbro M. Subatmospheric pressure in the rabbit pleural lymphatic network. J Physiol. 1999; 520:761–769. [PubMed: 10545142]
19. McMaster PD. The relative pressures within cutaneous lymphatic capillaries and the tissues. J Exp Med. 1947; 86(4):293–308. [PubMed: 19871679]
20. Nathanson SD, Mahan M. Sentinel Lymph Node Pressure in Breast Cancer. Ann Surg Oncol. 2011
21. Burton-Optiz R, Nemser R. The Viscosity of Lymph. Am J Physiol. 1917; 45:25–29.

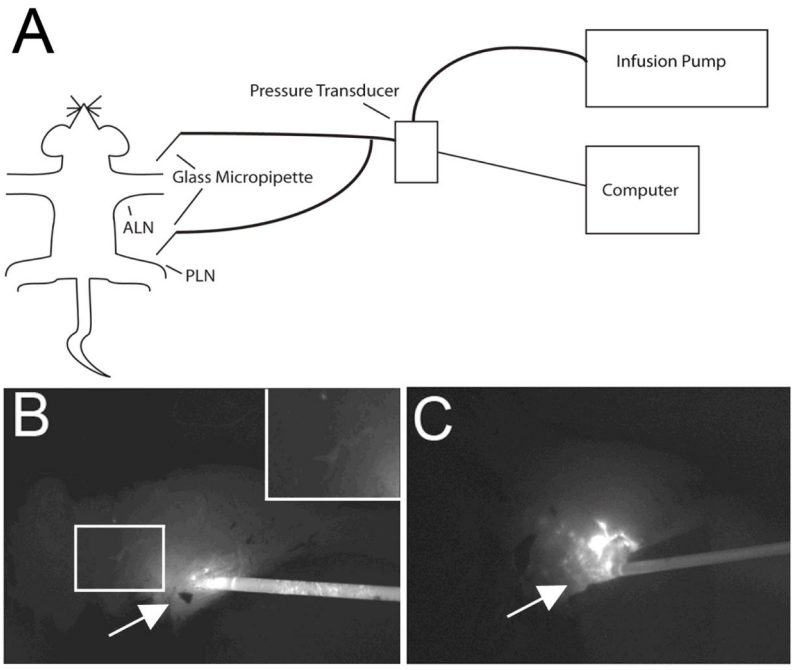

Figure 1. Schematic diagram of a mouse instrumented with the PLN and ALN pressure measurement system and NIR imaging to detect leakage

Mice are anesthetized with isoflurane, placed on a heated surgery table, and Evan's blue dye is injected into the hind footpad or front paw, respectively. 20 minutes later, a surgical incision is made to expose either the PLN or ALN, and the ICG filled borosilicate glass micropipette connected to the pressure transducer and infusion pump is placed into the lymph node. The pressure measurement is then obtained without flow from the pump. To confirm proper placement of the micropipette, the ICG flow into the lymph node during increasing pressure from the infusion pump is monitored by NIR imaging. A schematic representation of this procedure is presented (A). Only pressure measurements from lymph nodes that have not been ruptured by the glass micropipette are recorded. This is evident in non-leaking nodes (~80% of injections) by a limited residue ICG signal at the injection site (solid arrow in B), versus the gross ICG leakage of a ruptured node (solid arrow in C). ICG can be seen upstream in lymph nodes that have been successfully injected with ICG (inset in B).

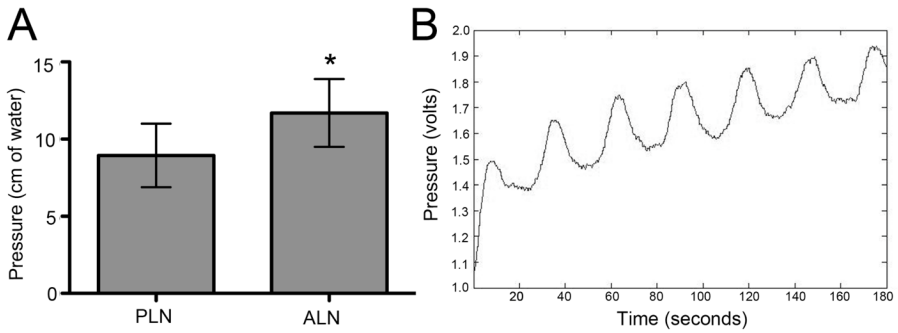

Figure 2. ***In vivo*** **axillary and popliteal lymph node pressure measurements**

In vivo pressure measurements of axillary and popliteal lymph nodes of mice (n=8 for PLN, n=7 for ALN) were obtained using the methods described in Figure 1. (A) The data are presented as the mean ± SD (*p <0.05 vs. PLN). Occasionally, a pulse in the pressure measurement could be detected, indicating direct placement of the micropipette into a lymphatic channel as evidenced by a sinusoidal curve of the rhythmic lymphatic pulse (B).

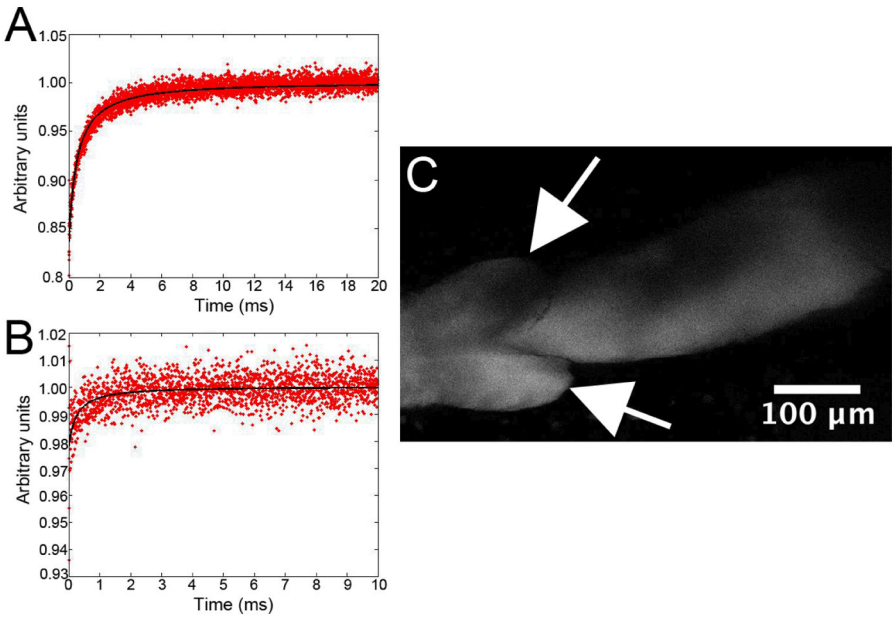

Figure 3. MP-FRAP approach to measure *in vivo* viscosity of lymph in lymphatic vessels afferent to PLN

First MP-FRAP plots of a 1mg/ml *in vitro* solution of FITC-BSA are acquired (normalized fluorescence photon counts, F_T/F_0) (**A**). Then *in vivo* MP-FRAP plots are acquired from FITC-BSA loaded lymphatic vessels afferent to PLN. For the *in vivo* MP-FRAP**,** 30µl of 1mg/ml FITC-BSA was injected into the hind footpad, and lymphatic vessels were surgically exposed >2hr later, followed by MP-FRAP (**B**). A two-photon image of the FITC-BSA loaded lymphatic vessel, from which MP-FRAP data was obtained, is shown (Arrows indicate the valves in the lymphatic vessel) (**C**).